frontiers in Materials

ORIGINAL RESEARCH
published: 19 February 2020
doi: 10.3389/fmats.2020.00033

Three-Dimensional Cotton-Wool-Like Polyhydroxybutyrate/Siloxane-Doped Vaterite Composite Fibrous Scaffolds: Effect of Imogolite-Coating on Physicochemical and Cell Adhesion Properties

Akiko Obata[1], Kazuma Mori[1], Keiichi Inukai[2], Katsuya Kato[3], Gowsihan Poologasundarampillai[4]* and Toshihiro Kasuga[1]*

[1] Division of Advanced Ceramics, Nagoya Institute of Technology, Nagoya, Japan, [2] Department of Materials and Chemistry, Structural Materials Research Institute, National Institute of Advanced Industrial Science and Technology (AIST), Nagoya, Japan, [3] Department of Materials and Chemistry, Inorganic Functional Materials Research Institute, National Institute of Advanced Industrial Science and Technology (AIST), Nagoya, Japan, [4] School of Dentistry, Institute of Clinical Sciences, University of Birmingham, Birmingham, United Kingdom

Poly(3-hydroxybutyrate-co-4-hydroxybutyrate), P(3HB-4HB), and siloxane-doped vaterite (SiV) composite fibrous scaffolds with 3D cotton-wool-like structure were developed using an electrospinning system for use in bone tissue regeneration. Scaffolds exhibited a significantly larger fiber-fiber separation distribution than non-woven fiber mats as observed with micro-computed tomographic studies. Coating the hydrophobic P(3HB-4HB)/SiV fibers with imogolite nanotubes (INT), aluminum silicate nanotubes, made the 3D construct hydrophilic and improved water penetration into the 3D structure (~2 s). Coating efficacy was confirmed by the detection of aluminum on the surface of fibers using scanning electron microscopy (SEM) energy dispersive spectroscopy (EDS). Dissolution experiments showed increased release of silicate ions in cell culture medium which can improve migration and mineralization of osteogenic cells inside of the 3D structure. The coating also contributed to an enhanced adhesion and migration of osteoblast-like cells (SaOS-2) within the 3D construct. The differentiation and mineralization of the cells were not affected by the coating. The coating for such cotton-wool-like structured scaffolds was effective for an enhancement of cell functions on early stages of culture. Thus, the developed materials with 3D structure, flexibility, silicate-ion release ability, and cell compatibility are expected to be good candidate materials for bone tissue regeneration.

Keywords: cotton-wool like structure, polyhydroxyalkanoates, imogolite, electrospinning, cell adhesion, 3D μCT quantification

OPEN ACCESS

Edited by:
Francesco Baino, Politecnico di Torino, Italy

Reviewed by:
Ahmed El-Fiqi, Dankook University, South Korea
Saeid Kargozar, Mashhad University of Medical Sciences, Iran

****Correspondence:***
Akiko Obata
obata.akiko@nitech.ac.jp
Gowsihan Poologasundarampillai
G.Poologasundarampillai@bham.ac.uk

Specialty section:
This article was submitted to Biomaterials, a section of the journal Frontiers in Materials

Received: *04 October 2019*
Accepted: *30 January 2020*
Published: *19 February 2020*

Citation:
Obata A, Mori K, Inukai K, Kato K, Poologasundarampillai G and Kasuga T (2020) Three-Dimensional Cotton-Wool-Like Polyhydroxybutyrate/Siloxane-Doped Vaterite Composite Fibrous Scaffolds: Effect of Imogolite-Coating on Physicochemical and Cell Adhesion Properties. Front. Mater. 7:33. doi: 10.3389/fmats.2020.00033

INTRODUCTION

Poly(3-hydroxybutyrate-*co*-4-hydroxybutyrate), P(3HB-4HB), is a polyhydroxyalkanoate (PHA) which is a biodegradable natural thermoplastic. Several types of PHAs including P(3HB-4HB) have been developed for use in tissue regeneration (Türesin et al., 2001; Tokiwa and Calabia, 2004; Chen, 2009). In addition, composite materials containing P(3HB-4HB) have been developed for scaffold application (Zhou et al., 2017; Azuraini et al., 2019). PHAs as implant materials offers several benefits; (1) *in vivo,* PHAs degrade into less acidic and less inflammatory products than synthetic resorbable polymers, such as poly(L-lactic acid) (PLLA); (2) the products of degradation are present in blood and tissue hence PHAs are not harmful to body (Qu et al., 2006; Ying et al., 2008). P(3HB-4HB) is a copolymer consisting of poly 3-hydroxybutyrate (PHB) and poly 4-hydroxybutyrate (P4HB) and has a statistically random distribution of PHB and P4HB units.

The biodegradability and mechanical property of P(3HB-4HB) depends heavily on the 4HB content in the copolymer (Saito and Doi, 1994). Saito et al. showed that the elongation to failure of P(3HB-4HB) with 82 mol% 4HB was 1,320% and, when 4HB content was 3 mol%, the elongation to failure dropped to 45%. While, the elongations to failure of polymers PHB and P4HB are 5 or 1,000%, respectively. The ability to tune the physical property and *in vivo* durability of P(3HB-4HB) by varying the 4HB content in the copolymer makes it a useful material for development of scaffolds (Obata et al., 2013a; Nishizuka et al., 2014; Vigneswari et al., 2016; Maksimcuka et al., 2017; Zhijiang et al., 2017).

Cotton-wool-like structured materials have been developed and reported in the last 10 years. (Schneider et al., 2008a,b; Yokoyama et al., 2009; Kasuga et al., 2012; Obata et al., 2013b; Poologasundarampillai et al., 2014; Mandakhbayar et al., 2018; Norris et al., 2020) Owing to their three-dimensional fibrous structure, they have high porosity, few fiber-fiber contact points, large space between fibers, flexibility, and easy-handling. Hence they have potential to be used as filler materials. In our previous work, the composites consisting of PLLA and siloxane-dope vaterite (SiV) with a cotton-wool-like structure were prepared by electrospinning with our home-made system (Kasuga et al., 2012; Obata et al., 2013b). Electrospinning is a versatile technique for producing nano- and micro-fibers and has been successfully employed in the production of biomaterials for regenerative medicine (Doostmohammadi et al., 2020) Silicate and calcium ions are released from the SiV component of the composite, which enhances mineralisation by osteoblast-like cells. The cells are able to migrate into inside of the cotton-wool-like structures. However, not only cell suspension but body fluids hardly permeates inside of the cotton-wool-like structure via gaps between fibers by just dripping the material inside the fluids. This is due to the surface hydrophobicity from the polymer fibers. Tissue integration of PHA is expected to be enhanced by resolving this issue.

Hydrophilicity and osteoblast-like cell adhesion in 3 h on PLLA/SiV fibremat (non-woven) were successfully enhanced by coating the fibers with imogolite nanotubes (INTs) (Yamazaki et al., 2012). INTs are aluminum silicate nanotubes, $(HO)_3Al_2O_3Si(OH)$, consisting of a nanotubular structure of ∼2.2 nm external and ∼1.0 nm internal diameters (Cradwick et al., 1972) and up to several hundreds of micrometers in length. INTs are hydrophilic because they have numerous hydroxyl groups on their surfaces. In addition, they have been reported to exhibit a high protein adsorption property because of their high surface area (Ishikawa et al., 2009). Thus, the INTs coated on the fiber surfaces were expected to facilitate protein adsorption, which then lead to enhanced cell adhesion on the PLLA/SiV fibers.

Aims of the present work were to fabricate cotton-wool-like structured composite materials consisting of PHA/SiV with the electrospinning method and to evaluate effects of INT-coating on the adhesion of osteoblast-like cells on the materials. Tomographic imaging was performed to observe the differences in fibrous structures between the cotton-wool-like structure and non-woven fiber mat. The effect of INT coated-fiber surfaces on cell adhesion was evaluated by culturing osteoblast-like cells on the materials using a culture medium with or without serum proteins which are involved to the cell adhesion.

MATERIALS AND METHODS

Preparation of P(3HB-4HB)/SiV Composites With a Cotton-Wool-Like Structure

Composites of P(3HB-4HB) (4HB: 18 ml%, G5, Singapore) and SiV particles (Si content: 2.0 wt.%, Yabashi Industries Co., Ltd., Japan) were prepared by melt-kneading at 110°C for 10 min. The ratio of P(3HB-4HB:SiV was 7:3 in weight. The resulting composite pellets were dissolved in chloroform (Wako Pure Chemicals, Japan) to 10 wt.% P(3HB-4HB) concentration and electrospun at the following conditions, electrical voltage: 8 kV, tip to collector distance: 300 mm, feeding rate: 0.050 mL/min, needle size: 0.8 mm in diameter. Ethanol (Wako Pure Chemicals, Japan) in a glass bath was used as a collector (Kasuga et al., 2012). The prepared composite samples with a cotton-wool-like structure are denoted by "PHA/SiV," hereafter. For the tomographic imaging, PHA/SiV fibremat (non-woven) was fabricated using the same composite solution by electrospinning with a drum-shaped collector (Maksimcuka et al., 2017). The fibromat samples are denoted by "2D fibremat," hereafter.

Imogolite Nanotube Coating for PHA/SiV

Imogolite nanotubes (INTs) were synthesized following the method described by Suzuki et al. (2007). A quantity of 18.47 g of aluminum chloride (Wako Pure Chemicals, Japan) and 9.2 g of sodium silicate (Wako Pure Chemicals, Japan) were dissolved in 500 mL of distilled water. The Si/Al molar ratio was 0.41. To set the pH of the resulting solution, 1 *M* sodium hydroxide (Wako Pure Chemicals, Japan) aqueous solution was added to it at a rate of 2 mL/min. Centrifugation and rinse with distilled water were performed for the resulting solution and repeated three times. The sample pellets obtained after the final centrifugation was dispersed in 12 L of distilled water. Twelve milliliter of 5

M hydrochloric acid (HCl, Wako Pure Chemicals, Japan) was added to the prepared solution to acidify and then heated at 95°C, resulting in formation of INTs with average length of 400 nm (**Figure S1**). The morphology of the prepared INT can be seen in our previous report (Yamazaki et al., 2012). The INTs stock solution was prepared by dispersing the INTs in distilled water (0.087 wt.%). The INTs suspension for coating PHA/SiV was obtained by mixing the stock solution with distilled water (10 wt.% of the stock solution). Five milligram of PHA/SiV was dipped in the INTs suspension for 5 s with a pulling speed of 0.5 mm/s and then dried at room temperature in vacuum for 1 h. The coating for PHA/SiV was repeated 3, 4, or 5 times, resulting in the preparation of INTs-coated PHA/SiV (denoted by INT/PHA/SiV) with varied amounts of INTs on fibers of PHA/SiV surfaces. For cell culture tests, the INT/PHA/SiV after 4 repeating was used. The INT/PHA/SiV before and after immersion in a cell culture medium were observed by scanning electron microscopy (SEM, JCM-6000, JEOL, Japan) incorporating energy dispersive spectrometry (EDS) after coating with amorphous osmium using a osmium coater (NeocST, Meiwafosis Co., Ltd., Japan).

Micro-Computed Tomographic (μCT) Studies of Material Structures

Fibremats were scanned using synchrotron-radiation based in-line phase contrast μCT at the Diamond Light Source (DLS), Diamond Manchester Branchline (DMB) (Rau et al., 2011; beamtime MT11079-1). X-ray with energies in the range of 8–35 keV, filtered with 950 μm carbon and 500 μm aluminum were used to illuminate the samples. Transmitted X-rays were then imaged via $CdWO_4$-sintilator-coupled detector (PCO dimax S4, PCO AG, Germany) placed 200 mm from the sample. Samples were rotated from 0 to 180° at a step of size of 0.05° collecting in total 3,601 projections at 40 ms exposure. Projections were then reconstructed into 3D dataset using filtered back projection algorithm (Atwood et al., 2015). Obtained μCT data were then analyzed using Fiji® (Schindelin et al., 2012).

Image Processing and Analysis

Fiji (ImageJ, US) was used to process and analyse the data (Schindelin et al., 2012; Rueden et al., 2017). A 3D median filter was applied to remove noise. The 32 bit data was then converted into 8 bit and segmented to background or fibers. Segmentation was applied by first fitting Gaussian distributions for background and fibers on the total histogram of the data. The intersection point of the two distributions was taken as the threshold value. Porosity was calculated as a percentage of empty space of the total volume. Fiber diameter and fiber-fiber separation were calculated by applying Local Thickness (Hildebrand and Rüegsegger, 1997) routines on the segmented fibers and background, respectively. Calculated local thicknesses were exported into OriginPro® (OriginLab Corporation, US) and analyzed. ImageJ-Volume Viewer (ImageJ, US) plugin was used to produce the 3D images.

Evaluation of Rate of Water Penetration Within the Fibrous Scaffolds

To estimate hydrophilicity of cotton-wool-like structured samples, the time of water penetration on the samples was measured. To obtain flat top surface of the cotton-wool-like samples, discs with 6.0 mm in diameter of PHA/SiV or INT/PHA/SiV were molded. Then 50 μL of distilled water was dropped on the disc surface. The time for all the water to penetrate the disc samples was measured ($n = 5$).

Evaluation of Ion Release From Fibers in Cell Culture Media

Ten mg of PHA/SiV or INT/PHA/SiV were soaked in 70% ethanol solution for 10 min for sterilization and then dried in a laminar flow cabinet for 1 h. The dried samples were soaked in 4 ml of McCoy' 5A (Gibco, Thermo Fisher Scientific Inc., US) supplemented with 10 vol% fetal bovine serum (FBS) and 1 vol% penicillin-streptomycin (Wako Pure Chemicals, Japan) following filtration with 0.2 μm polytetrafluoroethylene filters. They were incubated at 37°C for 3–168 h in a CO_2 incubator with 5% of CO_2 ($n = 3$). Concentrations of Ca, Si and P elements in the culture media were measured by inductively coupled plasma-atomic emission spectroscopy (ICP-AES, ICPS-7000, Shimadzu, Japan). The samples after the immersion for 168 h were rinsed with distilled water and then dried at room temperature in air. They were characterized with X-ray diffractometer (XRD, X'pert, Philips, US) and observed by SEM after coating with amorphous osmium.

Evaluation of Cell-Material Interactions Using Human Osteoblast-Like Cells (SaOS-2)

Five mg of PHA/SiV or INT/PHA/SiV was shaped using a stainless mold with 6.0 mm in diameter and 0.24 mm in height. The molded samples were sterilized with the above-mentioned method and then placed in 96 well plates (Thermo Fisher Scientific, Japan). The McCoy' 5A culture media with and without FBS were used to estimate influence of the INTs coating on cell adhesion via protein adsorption onto sample surfaces. The McCoy' 5A culture medium without FBS was prepared with the above-mentioned, except adding FBS. SaOS-2 cell suspension was prepared using the culture media with or without FBS and then seeded on the samples placed in 96 well plates (30,000 cells/well). The well plate (without any samples) was used as control sample. They were incubated at 37°C for 6 h in a CO_2 incubator with 5% of CO_2 ($n = 3$).

Live cell numbers on/in the samples were estimated by measuring their metabolic activities using Cell Counting Kit-8 (Dojindo, Japan) following manufacturer's instructions. After 6 h of culture, the samples were taken out and placed in new well plates and then rinsed with phosphate buffer solution (PBS, pH = 7.4). A 100 μL of fresh culture medium and 10 μL of a reagent solution of the kit was added into each well and then incubated for 2 h. The metabolic activities were evaluated by measuring the absorbance of the resulting medium at 450 nm with a microplate reader (SUNRISE Remote, TECAN, Switzerland).

Morphology of the cells on the samples after 6 h of culture was observed by SEM. The samples after culture was rinsed with PBS twice and then fixed with 2.5 vol% glutaraldehyde (Wako Pure Chemicals, Japan) for 40 min at 4°C. They were dehydrated through a series of increasing concentrations of ethanol and, finally, dried with hexamethyldisilazane (Wako Pure Chemicals, Japan). SEM observation was carried out for the sample coated amorphous osmium.

Cell proliferation, differentiation, and mineralization were examined after culturing for maximum 30 days. The used well plate, incubating conditions, cell density, and sample numbers were the same with the aforementioned one. The McCoy' 5A culture medium with FBS, the proliferation medium, was used until day 7. After day 7, the differentiation medium, which is the proliferation medium supplemented with 10 nM ascorbic acid, 50 μM disodium glycerophosphate 5.5 hydroate, and 10 nM dexamethasone (all chemicals are of Wako Pure Chemicals, Japan), was used until the end of the culture. The medium was changed every other day. For the proliferation test, the number of live cells were counted using Cell Counting Kit-8. For the differentiation test, alkaline phosphatase activity (ALP activity) in the cells was measured using *p*-nitrophenyl phosphate tablets (Sigma-Aldrich Corporation, USs) in accordance with the manufacture's instructions. ALP activity was estimated by measuring the absorbance of the resulting medium at 400 nm, and cell number was estimated as described above. For the mineralization test, calcium deposition amount was evaluated. One mL of HCl solution (2 *M*) was added to the well to dissolve the minerals. Calcium in the well was then measured using the Calcium E test (Wako Pure Chemicals, Japan), in accordance with the manufacture's instructions.

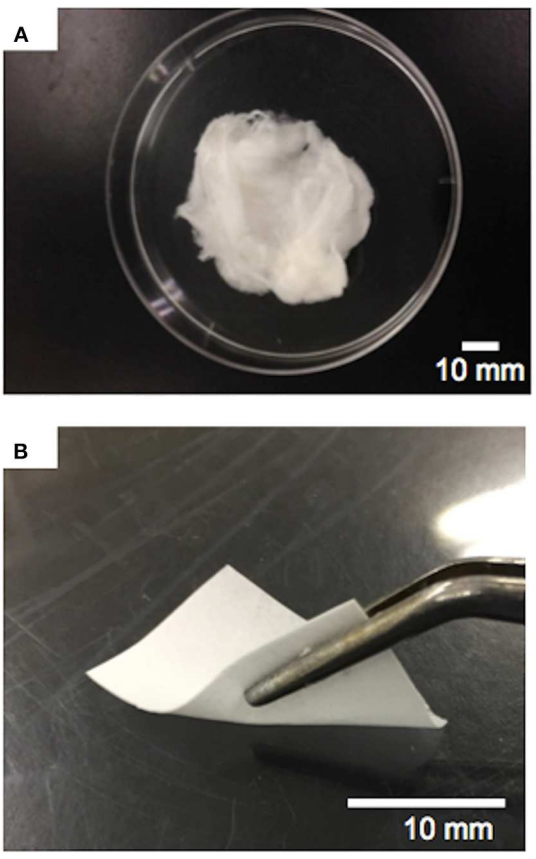

FIGURE 1 | Appearance of INT/PHA/SiV with cotton-wool-like structure **(A)** and fibremat **(B)**.

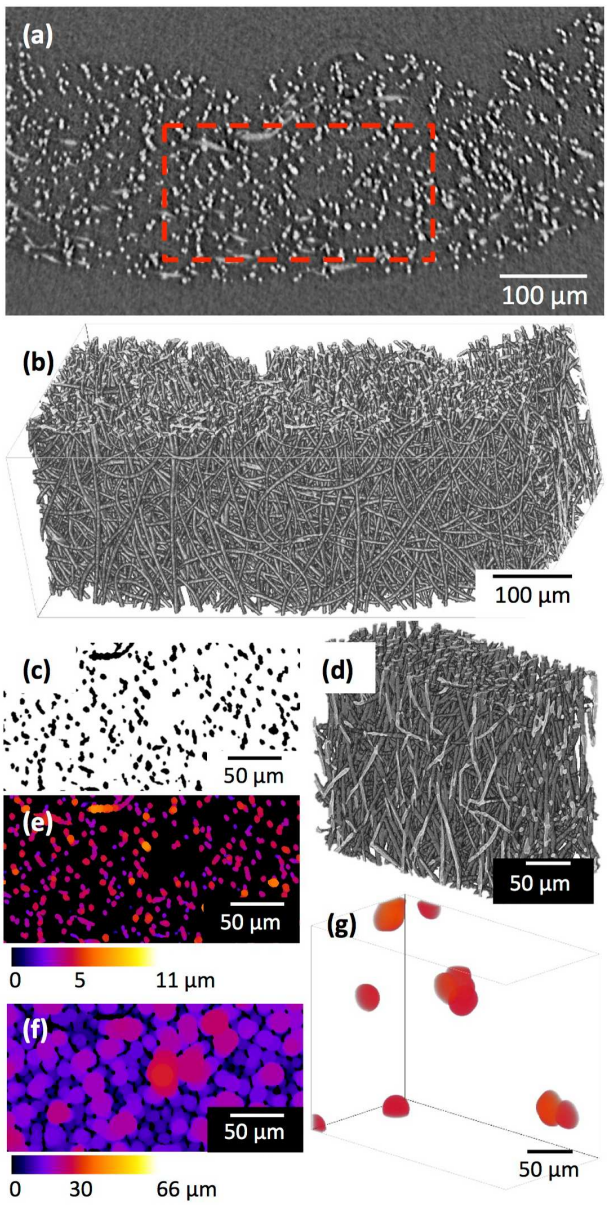

FIGURE 2 | μCT images and analysis of the 2D fibremat: a single 2D slice **(a)** after 3D median filter and 3D rendering **(b)** of **(a)**. A small volume (red box in **a**) was extracted and binarized, **(c)** 2D slice after binarization and **(d)** 3D rendering of **(c)**. Fiber diameter **(e)** and fiber-fiber separation **(f,g)** were quantified by performing a local thickness calculation. **(g)** Shows 3D rending of fiber-fiber separation in **(d)** that is >25 μm size.

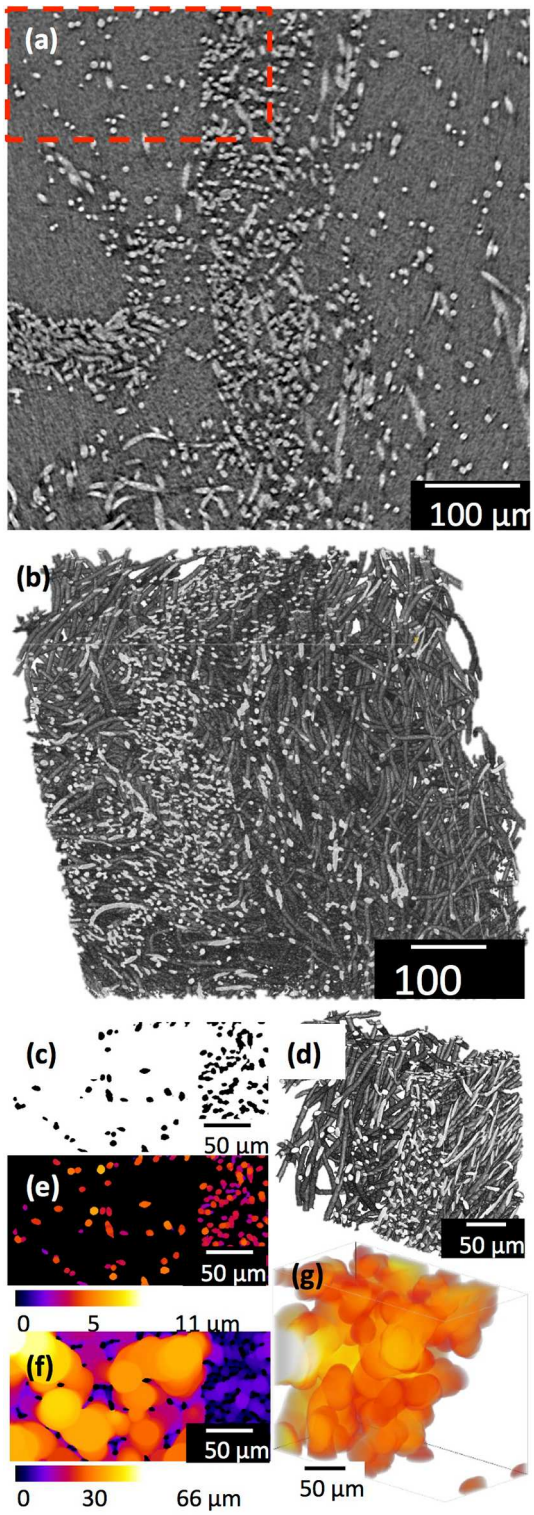

FIGURE 3 | µCT images and analysis of the 3D cotton-wool-like: a single 2D slice **(a)** after 3D median filter and 3D rendering **(b)** of **(a)**. A small volume (red box in **a**) was extracted and binarized, **(c)** 2D slice after binarization and **(d)** 3D rendering of **(c)**. Fiber diameter **(e)** and fiber-fiber separation **(f,g)** were quantified by performing a local thickness calculation. **(g)** Shows 3D rending of fiber-fiber separation in **(d)** that is >25 µm size.

Statistical Analysis

The data were presented as the mean ± standard deviation (SD). Statistical analysis was performed using Student's *t*-test for the data of samples with and without INT coating. Values with $p < 0.05$ were considered to be significant.

RESULTS AND DISCUSSION

Three-Dimensional Structure of the Composites

Figure 1 shows the (a) 3D cotton-wool-like and (b) 2D fibremat structure of INT/PHA/SiV. INT/PHA/SiV maintained the fluffy 3D cotton-wool-like structure even after 4 times dip coating with INT. The composite materials were observed to have an excellent mechanical property derived from the nature of PHA (**Figure S2**). MicroCT was used to image the 3D structures of

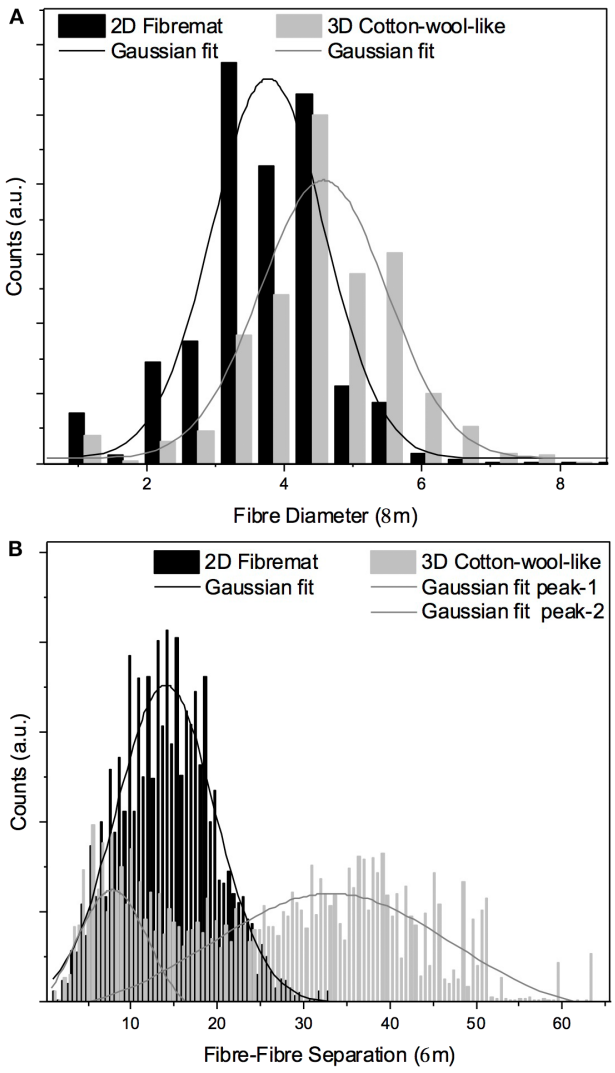

FIGURE 4 | Fiber diameter **(A)** and fiber-fiber separation **(B)** calculated from µCT images from the 2D fibremat and 3D cotton-wool-like materials.

the electrospun materials (**Figures 2–4**). Synchrotron-based in-line phase contrast μCT is a powerful method to image the 3D structures of electrospun polymeric materials under both static and dynamic conditions (Maksimcuka et al., 2017). **Figures 2**, **3** show the microCT images and quantification of the fiber morphologies of the fibremat and cotton-wool-like samples. The 3D images show that the scaffolds have a homogenous fiber

TABLE 1 | Summary of the porosity, modal fiber diameter and modes of fiber-fiber separation calculated from μCT images for both the 2D fibremat and 3D cotton-wool-like materials.

	2D Fibermat	3D Cotton-wool-like	
Porosity	84.8	86.6	
Fiber (%) diameter (μm)	3.77 ± 0.08	4.57 ± 0.08	
Fiber-fiber separation (μm)	14.0 ± 0.16	7.86 ± 0.43	33.2 ± 0.85*

**The 3D cotton-wool-like structured material has a bi-modal fiber-fiber separation.*

TABLE 2 | Time of water penetration into samples.

The number of coating	Time of water penetration into samples (s)
0	No penetration
3	~10 ± 3
4	~3 ± 1
5	~2 ± 2

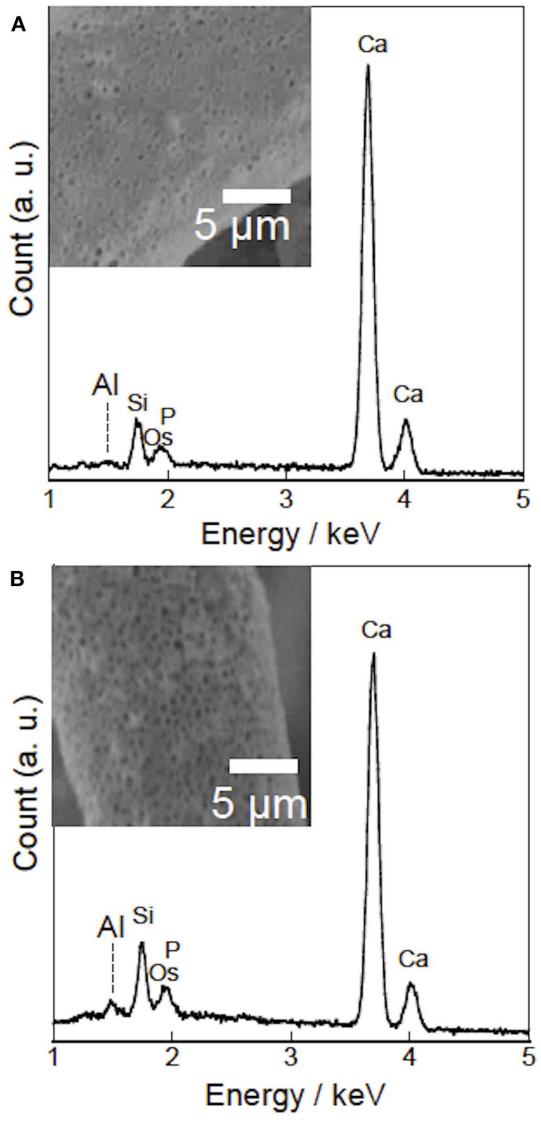

FIGURE 5 | SEM-EDS analysis of PHA/SiV **(A)** and INT/PHA/SiV **(B)**. Insets show SEM images of fiber surfaces (**A**-inset) before and (**B**-inset) after INT coating.

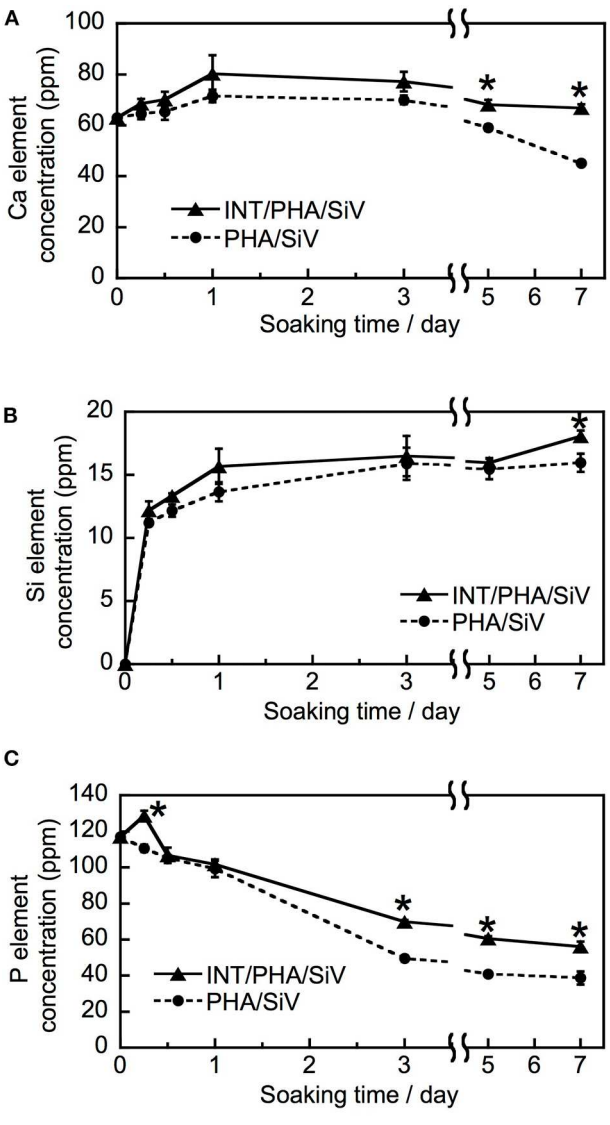

FIGURE 6 | Ion release behavior of PHA/SiV and INT/PHA/SiV in cell culture medium. Plots of Ca **(A)**, Si **(B)**, and P element **(C)**. $n = 3$. * $p < 0.05$ compared to PHA/SiV at the same time point.

diameter. Fiber diameter was calculated by performing a Local Thickness routine on ImageJ (**Figures 2e**, **3e**). **Figure 4A** shows the plot of the distribution of fiber diameters for both materials and the modal fiber diameter is summarized in **Table 1**. The fiber diameter for the 2D fibremat and 3D cotton-wool-like materials had a narrow distribution centered around 3.77 and 4.57 μm, respectively. The images clearly illustrate the difference in packing of the fibers from a 2D fibremat (**Figure 2**) to a 3D cotton-wool like (**Figure 3**) structure. The 2D slice (**Figures 2a,c**) and 3D rendering (**Figures 2b,d**) show qualitatively that in the case of 2D fibremat the fibers are closely packed together and are evenly spaced apart into a thin sheet. While, the 3D cotton-wool-like structured material has an inhomogeneous packing of the fibers (**Figures 3a–d**). **Figures 2f,g 3f,g** show the fiber-fiber separation in 2D and 3D. It is clear from these images that the fiber-fiber separation for 2D fibremat is homogeneous while that for the 3D cotton-wool-like material is inhomogeneous. **Figure 4B** shows the distributions of fiber-fiber separations. The 2D fibremat has a narrow distribution with modal fiber-fiber separation distance of 14.0 μm with a range of 1–28 μm. While the 3D cotton-wool-like material has a bimodal distribution with modes at 7.86 and 33.2 μm and a range of 1–67 μm. Although the porosity for 3D cotton-wool-like material (86.6%) is only 2.2% higher than the 2D fibremat (84.8%), the pore-size is much greater. However, this pore distribution in 3D space is inhomogeneous. Further work is required to improve the structural homogeneity of the 3D cotton-wool-like material. **Figure 5** shows SEM images of the surface of a single fiber of INT/PHA/SiV and PHA/SiV as well the EDS results for each. Although no difference in the morphology of the surface was observed between the two samples, Al on the surface of INT/PHA/SiV was confirmed. Since, Al on the surface was <0.3 atm%, a thin INT-coating was expected to be formed. INT assembles into thin fibers with high aspect ratio (Suzuki et al., 2007; Yamazaki et al., 2012), therefore the coating on the PHA surface is likely to be electrostatically bonded entangled fibrous mesh (**Table S1**).

Hydrophilicity and Ion Release From Fibers

Hydrophilicity of PHA/SiV was drastically increased after the INT-coating, as demonstrated by the data presented in **Table 2**. The time required for water to penetrate into the PHA/SiV cotton-wool-like material decreased with increasing number of dip-coating with INT. From an initially non-absorbing material

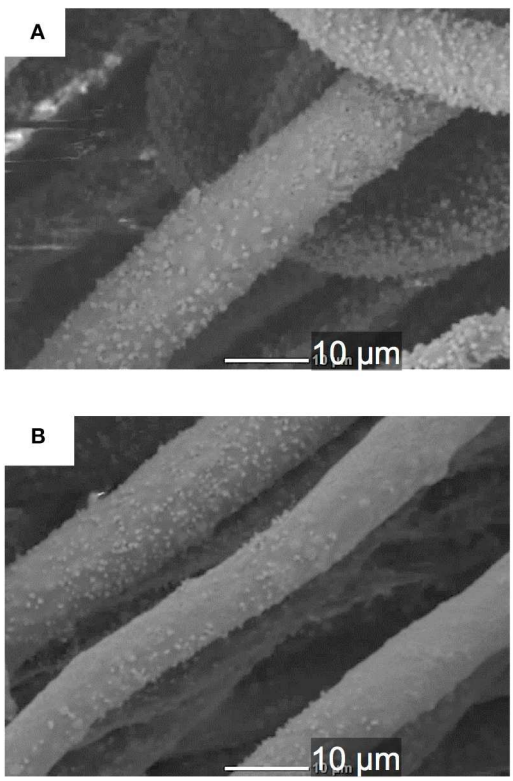

FIGURE 7 | SEM images of single fibers of PHA/SiV **(A)** and INT/PHA/SiV **(B)** after being soaked in cell culture medium for 7 days.

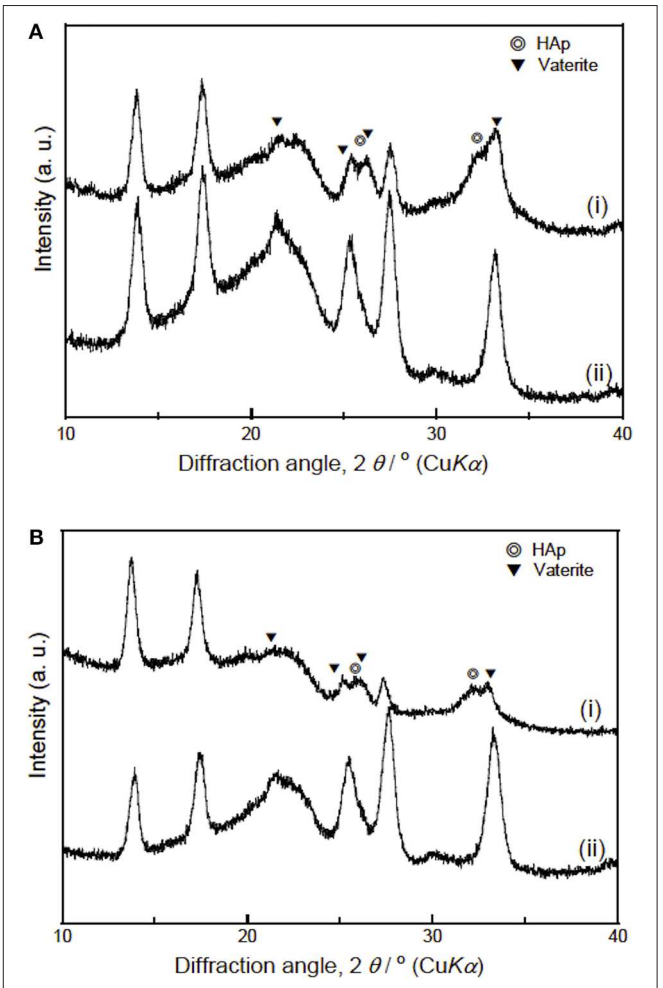

FIGURE 8 | XRD patterns of PHA/SiV **(A)** and INT/PHA/SiV **(B)** samples (i) after being soaked in cell culture medium for 7 days and (ii) before soaking. Assignments for vaterite was based on vaterite P63/mmc space group (JCPDS no. 33-0268) and for hydroxyapatite (HA-PDF File no- 00-009-0432).

to wicking up water in 2 ± 2 s after five dip-coating cycles. This means that the loading of INT on fibers of the samples contributed to the enhanced hydrophilicity. Further, the samples after coating for four times were as effective at wicking the water as those coated five times therefore number of coating cycles was kept to 4 for the entire study.

The results of the immersion tests using cell culture media (**Figure 6**) demonstrates that the silicate ion release from the samples was enhanced by the INT-coating. This indicates that water infiltration/access to SiV in/on the samples was promoted since their hydrophilicity was improved after the INT-coating, which accelerated the dissolution of SiV. Although calcium and phosphate ions were present in the culture medium used for the immersion test, the concentrations of the two ions after soaking INT/PHA/SiV were significantly higher than PHA/SiV, especially after 3 days of soaking. Calcium ion release was also expected to be enhanced after the INT-coating, since Ca^{2+} ion is also present in SiV, and the silicate ion release was accelerated after the coating as previously mentioned. The concentration of calcium and phosphate ions gradually decreased

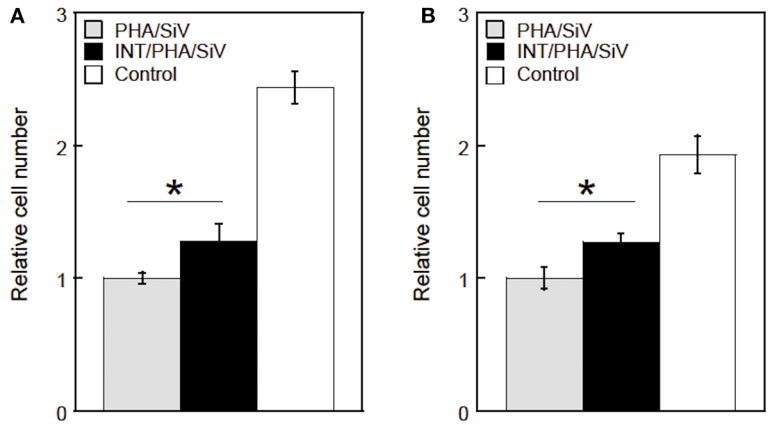

FIGURE 9 | Relative cell numbers on/in PHA/SiV or INT/PHA/SiV with cotton-wool-like structure after culturing in a culture medium supplemented with FBS **(A)** or non-supplemented **(B)**. $n = 3$. $^*p < 0.05$.

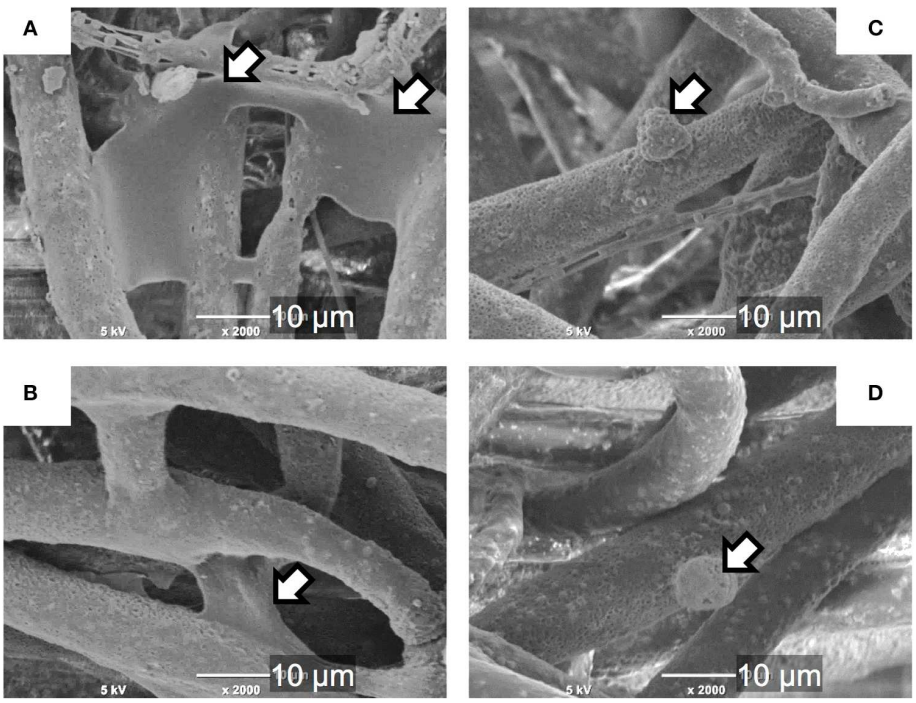

FIGURE 10 | SEM images of the cells on single fibers of PHA/SiV **(A,C)** or INT/PHA/SiV **(B,D)** after culturing in a culture medium supplemented with FBS **(A,B)** or non-supplemented **(C,D)**. Arrows in images indicate cells.

in 7 days; this was due to the formation of hydroxyapatite (HAp), on the surface of the fibers. This is supported by the SEM images and XRD patterns of the samples after 7 days of soaking in the culture medium (**Figures 7**, **8**). The concentration of calcium and phosphate ions were higher for INT/PHA/SiV than PHA/SiV. This indicates that there may exist difference in the amount of HAp precipitated between the two samples.

INT release into media after soaking the fibers was also analyzed. Al was not detected in ICP-AES measurements, although Al was observed on the fibers prior to soaking using EDS analysis (**Figure 5**). This decreased from ∼0.3 atm% to <0.1 atm% after soaking in media (**Figure S3**). This suggest only a negligible amount of INT was present on the fibers after 7 days in media. However, we expect the release behavior to be different *in vivo* from adsorption of protein (Wang et al., 2012) and limited diffusion.

Osteoblast-Like Cell Interactions to Fibrous Scaffolds

Results of the cell culture tests revealed that the INT-coating accelerated the cell adhesion on the cotton-wool-like structured samples, irrespectively the presence of proteins which mediated the cell attachment (**Figures 9**, **10**). This is because the INTs on the fiber surfaces exhibit an excellent protein adsorption ability owing to its large surface area (Ishikawa et al., 2009). In addition, the migration of the cells into inside of the samples was promoted due to the enhanced hydrophilicity of INT/PHA/SiV, as shown in **Table 1**. Generally, cell adhesion is mediated with integrins which is the major family of cell surface receptors. Integrins on extracellular surface of cell membranes bind ligands in extracellular matrix, e.g., fibronectin and vitronectin (Clark and Brugge, 1995). These proteins are found in FBS. Ishikawa et al. (2009, 2010) reported that substrates coated with various amounts of INTs promoted cell spreading and the proliferation and mineralisation of SaOS-2 and MC3T3-E1 cells. Therefore, such protein adsorption on the substrates coated with INTs led to the enhanced adhesion, irrespectively the substrate's shapes (cotton-wool-like structure or dense film). The cell adhesion was enhanced for the dense film of INT/PHA/SiV in comparison with that of PHA/SiV (**Figure S4A**). In the case of the culturing without FBS (**Figure 9B**), the cell number was enhanced on INT/PHA/SiV. Fiber surfaces of PHA/SiV shows hydrophobic due to the intrinsic property of PHA, which inhibit the penetration of cell suspension into inside of the cotton-wool-like structure. This caused a poor cell migration in PHA/SiV, especially in a short time, such as 6 h. The reason why the cell number was almost the same between INT/PHA/SiV film and PHA/SiV film (**Figure S4B**) is hydrophobic/hydrophilic property of sample surfaces had a minor influence on the cell adhesion since these substrates had a 2D flat surface and dense structure, and therefore penetration of the cell suspension was not possible. From the cell morphology shown in **Figure 10D**, even though the cell number in INT/PHA/SiV was higher than that in PHA/SiV, the cells on both the sample

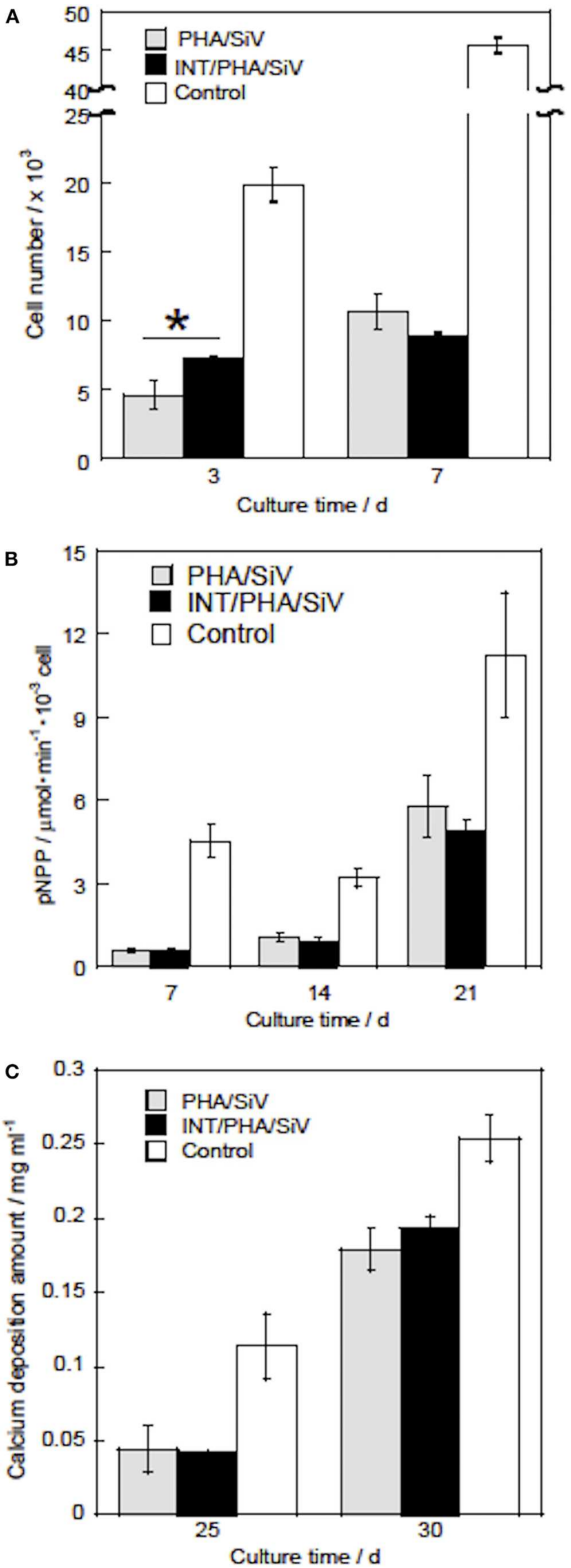

FIGURE 11 | Live cell numbers **(A)**, ALP activity **(B)**, and calcium deposition amounts **(C)** of the cells after culturing with PHA/SiV and INT/PHA/SiV). $n = 3$. $^*p < 0.05$.

surfaces seemed to be unhealthy as they possessed a round shape. On the other hand, the cells were observed to spread well when they were cultured in the medium supplemented with FBS.

The results of the proliferation test demonstrated that more live cells proliferated in the INT/PHA/SiV in comparison with PHA/SiV (**Figure 11A**) until day 3. The live cell number, however, was almost the same between the INT/PHA/SiV and PHA/SiV at day 7. The ALP activity level and calcium deposition amount of the cells increased with the culture time and there was no significant difference between INT/PHA/SiV and PHA/SiV (**Figures 11B,C**). Therefore, the INT-coating for such cotton-wool-like structured scaffolds would contribute to enhancement of cell functions on early stages, such as adhesion and proliferation in a few days. In addition, the INT was found to have no negative influence on the differentiation and mineralization in the scaffolds. Although Ishikawa et al. reported that INTs promoted not only cell proliferation but also mineralization, we could not observe such tendency in the present work. This may be due to different scaffold structure; the proliferation of the cells was enhanced until day 7, in the case of the INT/PHA/SiV film (**Figure S5**).

CONCLUSION

Flexible 3D cotton-wool-like structured composite materials of PHA/SiV that could release silicate ion were fabricated with electrospinning system. The results of microCT demonstrated that there was the difference in packing of the fibers from a 2D fibremat to a 3D cotton-wool-like sample. In the case of 2D fibremat, the fibers are closely packed together and are evenly spaced apart into a thin sheet. The 3D cotton-wool-like structure was highly porous with large spaces between fibers; the distributions of fiber-fiber separations were larger than those of the 2D fibremat. Therefore, the 3D structure could facilitate the migration of cells within the fibrous material in comparison to the 2D fibremat. In addition, the hydrophobicity of composite PHA matrix, was overcome by a simple method of coating the fibers with INT. Cell culture on these INT coated-3D cotton-wool-like fibers demonstrates that the coating successfully induced cells to migrate inside the 3D structure. In addition, the INT coated on the fiber surface could have enhanced cell adhesion from increased adsorbed proteins. Therefore, the INT-coating for the PHA/SiV fibers was effective for achieving a high hydrophilic surface and enhancing cell migration in and adhesion on the fibrous scaffolds. The INT/PHA/SiV fibers with 3D cotton-wool-like structure were expected to be useful for the use in bone tissue regeneration.

DATA AVAILABILITY STATEMENT

All datasets generated for this study are included in the article/**Supplementary Material**. Requests for access to raw and processed tomographic data should be sent to g.poologasundarampillai@bham.ac.uk.

AUTHOR CONTRIBUTIONS

AO wrote up this manuscript, and designed the materials and the strategy of this work. KM performed the materials preparation and evaluations for them. KI and KK prepared and characterized imogolite. GP wrote up this manuscript and did 3D micro CT quantification. TK designed the materials and the methods for preparation and evaluations.

FUNDING

GP would like to acknowledge EPSRC grant EP/M023877/1.

ACKNOWLEDGMENTS

Synchrotron tomography experiment was performed on the Branchline I13-2 of the Diamond Light Source synchrotron in Oxfordshire, UK, on the beamtime MT11079. The authors would like to acknowledge Dr. Andrew Bodey for their contributions to making the beam time possible.

SUPPLEMENTARY MATERIAL

The Supplementary Material for this article can be found online at: https://www.frontiersin.org/articles/10.3389/fmats.2020.00033/full#supplementary-material

REFERENCES

Atwood, R. C., Bodey, A. J., Price, S. W. T., Basham, M., and Drakopoulos, M. (2015). A high-throughput system for high-quality tomographic reconstruction of large datasets at Diamond light source. *Philos. Trans. A Math. Phys. Eng. Sci.* 373:20140398. doi: 10.1098/rsta.2014.0398

Azuraini, M. J., Huong, K. H., Abdul Khalil, H. P. S., and Amirul, A. A. (2019). Fabrication and characterization of P(3HB-*co*-4HB)/gelatin biomimetic nanofibrous scaffold for tissue engineering application. *J. Polym. Res.* 26:257. doi: 10.1007/s10965-019-1925-z

Chen, G. Q. (2009). A microbial polyhydroxyalkanoates (PHA) based bio- and materials industry. *Chem. Soc. Rev.* 38, 2434–2446. doi: 10.1039/b812677c

Clark, E., and Brugge, J. (1995). Integrins and signal transduction pathways: the road taken. *Science* 268, 233–239. doi: 10.1126/science.7716514

Cradwick, P. D. G., Farmer, V. C., Russell, J. D., Masson, C. R., Wada, K., and Yoshinaga, N. (1972). Imogolite, a hydrated aluminium silicate of tubular structure. *Nat. Phys.* 240, 187–189. doi: 10.1038/physci240187a0

Doostmohammadi, M., Forootanfar, H., and Ramakrishna, S. (2020). Regenerative medicine and drug delivery: progress via electrospun biomaterials. *Mater. Sci. Eng. C* 109:10521. doi: 10.1016/j.msec.2019.110521

Hildebrand, T., and Rüegsegger, P. (1997). A new method for the model-independent assessment of thickness in three-dimensional images. *J. Microsc.* 185, 67–75. doi: 10.1046/j.1365-2818.1997.1340694.x

Ishikawa, K., Abe, S., Yawaka, Y., Suzuki, M., and Watari, F. (2010). Osteoblastic cellular responses to aluminosilicate nanotubes, imogolite using Saos-2 and

MC3T3-E1 cells. *J. Ceram. Soc. Jpn.* 118, 516–520. doi: 10.2109/jcersj2.118.516

Ishikawa, K., Akasaka, T., Nodasaka, Y., Ushijima, N., Kaga, M., Abe, S., et al. (2009). Physical properties of aluminosilicate nanotubes, imogolite, as scaffold and effect on osteoblastic mineralization. *Nano Biomed.* 1, 109–120. doi: 10.11344/nano.1.109

Kasuga, T., Obata, A., Maeda, H., Ota, Y., Yao, X., and Oribe, K. (2012). Siloxane-poly(lactic acid)-vaterite composites with 3D cotton-like structure. *J. Mater. Sci. Mater. Med.* 23, 2349–2357. doi: 10.1007/s10856-012-4607-5

Maksimcuka, J., Obata, A., Sampson, W. W., Blanc, R., Gao, C., Withers, P. J., et al. (2017). X-ray tomographic imaging of tensile deformation modes of electrospun biodegradable polyester fibers. *Front. Mater. Sci.* 4:43. doi: 10.3389/fmats.2017.00043

Mandakhbayar, N., El-Fiqi, A., Dashnyam, K., and Kim, H. W. (2018). Feasibility of defect tunable bone engineering using electroblown bioactive fibrous scaffolds with dental stem cells. *ACS Biomater. Sci. Eng.* 4, 1019–1028. doi: 10.1021/acsbiomaterials.7b00810

Nishizuka, T., Kurahashi, T., Hara, T., Hirata, H., and Kasuga, T. (2014). Novel intramedullary-fixation technique for long bone fragility fractures using bioresorbable materials. *PLoS ONE* 9:e104603. doi: 10.1371/journal.pone.0104603

Norris, E., Ramos-Rivera, C., Poologasundarampillai, G., Clark, J. P., Ju, Q., Obata, A., et al. (2020). Electrospinning 3D bioactive glasses for wound healing. *Biomed. Mater.* 15. doi: 10.1088/1748-605X/ab591d

Obata, A., Iwata, T., Maeda, H., Hirata, H., and Kasuga, T. (2013a). Preparation of poly(3-hydroxybutyrate-co-4-hydroxybutyrate)-based composites releasing soluble silica for bone regeneration. *J. Ceram. Soc. Jpn.* 121, 753–758. doi: 10.2109/jcersj2.121.753

Obata, A., Ozasa, H., Kasuga, T., and Jones, J. (2013b). Cotton wool-like poly(lactic acid)/vaterite composite scaffolds releasing soluble silica for bone tissue engineering. *J. Mater. Sc.i Mater. Med.* 24, 1649–1658. doi: 10.1007/s10856-013-4930-5

Poologasundarampillai, G., Wang, D., Li, S., Nakamura, J., Bradley, R., Lee, P. D., et al. (2014). Cotton-wool-like bioactive glasses for bone regeneration. *Acta Biomater.* 10, 3733–3746. doi: 10.1016/j.actbio.2014.05.020

Qu, X. H., Wu, Q., and Chen, G. Q. (2006). *In vitro* study on hemocompatibility and cytocompatibility of poly(3-hydroxybutyrate-co−3-hydroxyhexanoate). *J. Biomater.* 17, 1107–1121. doi: 10.1163/156856206778530704

Rau, C., Wagner, U., Pešić, Z., and De Fanis, A. (2011). Coherent imaging at the diamond beamline I13. *Phys. Status Solidi* 208, 2522–2525. doi: 10.1002/pssa.201184272

Rueden, C. T., Schindelin, J., Hiner, M. C., DeZonia, B. E., Walter, A. E., Arena, E. T., et al. (2017). ImageJ2: imageJ for the next generation of scientific image data. *BMC Bioinformatics* 18:529. doi: 10.1186/s12859-017-1934-z

Saito, Y., and Doi, Y. (1994). Microbial synthesis and properties of poly(3-hydroxybutyrate-co-4-hydroxybutyrate) in Comamonas acidovorans. *Int. J. Biol. Macromol.* 16, 99–104. doi: 10.1016/0141-8130(94)90022-1

Schindelin, J., Arganda-Carreras, I., Frise, E., Kaynig, V., Longair, M., Pietzsch, T., et al. (2012). Fiji: an open-source platform for biological-image analysis. *Nat. Methods* 9, 676–682. doi: 10.1038/nmeth.2019

Schneider, O. D., Loher, S., Brunner, T. J., Schmidlin, P., and Stark, W. J. (2008a). Flexible, silver containing nanocomposites for the repair of bone defects: antimicrobial effect against *E. coli* infection and comparison to tetracycline containing scaffolds. *J. Mater. Chem.* 18, 2679–2684. doi: 10.1039/b800522b

Schneider, O. D., Loher, S. J., Brunner, T. J., Uebersax, L., and Simonet, M., Grass, R. N., et al. (2008b). Cotton wool-like nanocomposite biomaterials prepared by electrospinning: *in vitro* bioactivity and osteogenic differentiation of human mesenchymal stem cells. *J. Biomed. Mater. Res. B Appl. Biomater.* 84B, 350–362. doi: 10.1002/jbm.b.30878

Suzuki, M., Sato, H., Ikeda, C., Nakanishi, R., Inukai, K., and Maeda, M. (2007). State change of imogolite according to heating duration on synthesizing: self-organization and characterization change of imogolite according to heathg duration. *J. Clay Sci. Soc. Jpn.* 46, 194–199. doi: 10.11362/jcssjnendokagaku1961.46.194

Tokiwa, Y., and Calabia, B. P. (2004). Degradation of microbial polyesters. *Biotechnol. Lett.* 26, 1181–1189. doi: 10.1023/B:BILE.0000036599.15302.e5

Türesin, F., Gürsel, I., and Hasirci, V. (2001). Biodegradable polyhydroxyalkanoate implants for osteomyelitis therapy: *in vitro* antibiotic release. *J. Biomater. Sci. Polym. Ed.* 12, 195–207. doi: 10.1163/156856201750180924

Vigneswari, S., Murugaiyah, V., Kaur, G., Abdul Khalil, H. P. S., and Amirul, A. A. (2016). Simultaneous dual syringe electrospinning system using benign solvent to fabricate nanofibrous P(3HB-co-4HB)/collagen peptides construct as potential leave-on wound dressing. *Mater. Sci. Eng. C.* 66, 147–155. doi: 10.1016/j.msec.2016.03.102

Wang, K., Zhou, C., Hong, Y., and Zhang, X. (2012). A review of protein adsorption on bioceramics. *Interface Focus* 2, 259–277. doi: 10.1098/rsfs.2012.0012

Yamazaki, S., Maeda, H., Obata, A., Inukai, K., Kato, K., and Kasuga, T. (2012). Aluminum silicate nanotube coating of siloxane-poly(lactic acid)-vaterite composite fibermats for bone regeneration. *J. Nanomater.* 2012:463768. doi: 10.1155/2012/463768

Ying, T. H., Ishii, D., Mahara, A., Murakami, S., Yamaoka, T., Sudesh, K., et al. (2008). Scaffolds from electrospun polyhydroxyalkanoate copolymers: Fabrication, characterization, bioabsorption and tissue response. *Biomaterials* 29, 1307–1317. doi: 10.1016/j.biomaterials.2007.11.031

Yokoyama, Y., Hattori, S., Yoshikawa, C., Yasuda, Y., Koyama, H., Takato, T., et al. (2009). Novel wet electrospinning system for fabrication of spongiform nanofiber 3-dimensional fabric. *Mater. Lett.* 63, 754–756. doi: 10.1016/j.matlet.2008.12.042

Zhijiang, C., Qin, Z., Xianyou, S., and Yuanpei, L. (2017). Zein/Poly(3-hydroxybutyrate-co-4-hydroxybutyrate) electrospun blend fiber scaffolds: preparation, characterization and cytocompatibility. *Mater. Sci. Eng. C* 71, 797–806. doi: 10.1016/j.msec.2016.10.053

Zhou, T., Li, G., Lin, S., Tian, T., Ma, Q., Zhang, Q., et al. (2017). Electrospun poly(3-hydroxybutyrate-co-4-hydroxybutyrate)/graphene oxide scaffold: enhanced properties and promoted in vivo bone repair in rats. *ACS Appl. Mater. Interfaces* 9, 42589–42600. doi: 10.1021/acsami.7b14267

Conflict of Interest: The authors declare that the research was conducted in the absence of any commercial or financial relationships that could be construed as a potential conflict of interest.